EXPANDING THE DATASET OF MARS ATMOSPHERIC RETRIEVALS FROM MGS TES USING LIMB-GEOMETRY BOLOMETER OBSERVATIONS

E. L. Mason, *Center for Space Science and Technology, University of Maryland Baltimore County, NASA/GSFC, Center for Research and Exploration in Space Science and Technology, Baltimore, MD, USA, (emily.mason-1@nasa.gov)*, **M. D. Smith**, *NASA Goddard Space Flight Center, Greenbelt, MD, USA*, **M. J. Wolff**, *Space Science Institute, Boulder, CO, USA.*

Introduction:

The Thermal Emission Spectrometer (TES) onboard the Mars Global Surveyor (MGS) was a thermal infrared spectrometer (6-50 µm) with additional broadband infrared (5-100 µm) and visible (0.3-3.0 µm) wavelength bolometers (Christensen et al., 1992; 2001). Beginning in March 1999, the MGS TES operated nearly continuously for almost three Martian Years (MY) serving as the primary source for information on the state of the Martian atmosphere. Throughout the MGS mission, TES bolometer data were taken simultaneously.

Over time, the neon lamp used for producing the interferogram, the primary raw output of the spectrometer, began to degrade, and by September 2004, the lamp could no longer provide sufficient signal to collect usable spectrometer data. However, TES continued to take observations using its visible and infrared band bolometers for nearly a full Martian Year (MY) after the spectrometer ceased observations. The extended bolometer-only dataset covers a period that includes the entire MY 27 dust storm season and most of the MY 28 aphelion cloud belt season (see Figure 1).
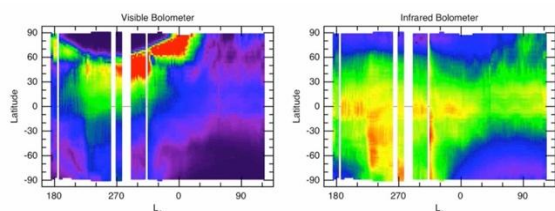
Figure 1: TES bolometer visible (left) and IR (right) brightness temperatures over the span of the bolometer-only observations

Previous studies have used the bolometer data to determine aerosol sizes (Clancy et al., 2003; 2010; Wolff and Pankine, 2016) and retrieve atmospheric temperatures between 60 and 100 km in altitude (Kutepov et al., 2008). These applications were limited to where coincident spectrometer data are available. Like the spectrometer data, the bolometer data contain important information about the state of the lower atmosphere. Limb-geometry infrared bolometer allows atmospheric retrievals of temperature and provides additional constraints on aerosol particle

size when combined with the visible bolometer. The thermal bolometer signal (right panel of Figure 1) clearly shows the seasonal patterns of temperature and aerosol optical depth. The visible bolometer (left panel of Figure 1) is sensitive to the scattering geometry of aerosols and requires radiative transfer modeling for interpretation.

Bolometer Dataset:

TES extended bolometer observations span the visible (0.3-3.0 µm) and infrared (5-100 µm) wavelength ranges and are available from MY 27, $L_s = 180°$ until MY 28, $L_s = 120°$. MGS was in a sun-synchronous, nearly polar orbit. For a single day, TES collected two sets of twelve strips of observations running from the north to south pole and spaced 29° apart in longitude. One set was taken near a local time of 2:00 PM (dayside) and the other was taken near 2:00 AM (nightside). During the period of bolometer-only operation, the observational sequence consisted of a pattern that alternated two orbits of nadir-only observations with two orbits of limb-only observations. This provided six complete pole-to-pole surveys of the limb each day at a wide range of longitudes with each individual limb scan spaced every 1.25° of latitude (Figure 2, left panel).
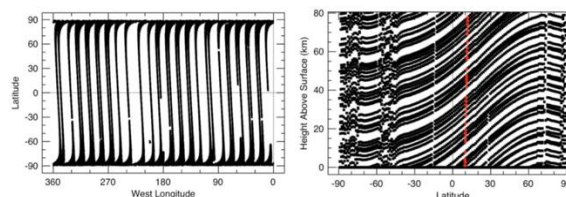
Figure 2: Bolometer observations in on a latitude-longitude map for six sols (left) and vertical distribution of observations (right).

Each orbit of bolometer-only observations devoted to limb scanning produced a set of observations like that shown in Figure 2, right panel. There are roughly 140 scans of the limb from pole to pole for both the daytime (~2:00 PM) and nighttime (~2:00 AM) portions of the orbit. The red points in Figure 2 are from one individual scan of the limb centered near 10° N latitude, and consist of roughly 35 measurements between the surface and a tangent height of 80 km. The projected size of a TES pixel at the limb

is 13 km.

Retrieval Algorithm: The retrieval algorithm combines limb-geometry visible and infrared bolometer observations with supplemental information obtained from nadir-geometry visible and infrared bolometer observations taken nearby in location and time. In the limb-viewing geometry, the signal from the visible bolometer is dependent on scattering into the line of sight. This signal is dependent on sunlight reflected from the surface, the viewing geometry, and the aerosol scattering properties, which include contributions from dust and ice particles. Only dayside observations are used in the retrieval algorithm. The signal observed by the thermal infrared bolometer is dependent on thermal emission from the atmosphere, surface, and aerosols as well as scattering. Night and day observations in the infrared are used.

Full multiple scattering is included in the radiative transfer model (Smith et al., 2013; McConnochie & Smith, 2008). The model uses a discrete ordinates method to treat scattering with 64 streams and 50 atmospheric layers set at 0.2 scale heights. Aerosol properties are taken from modeling results of Wolff et al. (2009), and gas absorption is included using the correlated-k approximation (Lacis & Oinas, 1991) with gas coefficients take from the HITRAN database (Gordon et al., 2017). Spherical geometry is treated within the code by a 'psuedo-spherical' approach where the curved path is defined by computing the correct limb-geometry emission angle for the path at the boundary of each layer.

The retrieval uses limb geometry from a single scan, which consists of 35 individual observations between the surface and 80 km), in conjunction with the nearest nadir-geometry bolometer observations in time and location. Aerosol optical depth and atmospheric and surface temperature are taken from TES climatology nadir observations as a first guess. Visible and infrared nadir observations are first used to retrieve surface albedo and temperature, respectively. Limb-geometry observations are used with the resulting surface albedo to derive vertical distributions of aerosol optical depth (from the visible bolometer), atmospheric temperatures, and column-integrated aerosol optical depth (from the infrared bolometer).
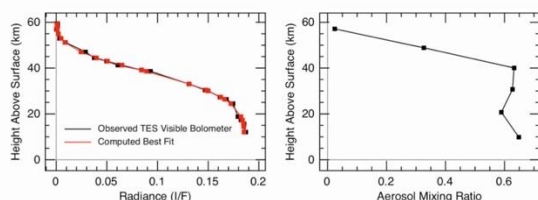
Figure 3: Example fit from MY 27, Ls = 246˚ at 29˚S latitude and 82˚ W longitude (Solis Planum).

The retrieval uses a chi-squared best fit metric to minimize radiance computed from the RT model as a function of height above the limb. Figure 3 shows the retrieval results for one dusty spectrum taken at MY 27, L_S=246°, 29° S latitude, 82° W longitude. The retrieval shows an excellent fit to the observation with the aerosol having a nearly uniform mixing up to a height of 40 km and declining rapidly above that level. The column extinction optical depth of the aerosol is 0.63 for dust at a wavelength of 9 μm.

Validation and Testing: Retrievals of atmospheric thermal and aerosol properties can be validated against concurrent MGS TES spectrometer limb and nadir observations during times when the spectrometer was operational. For nearly three Martian years, limb profiles were acquired every 10˚ or 20˚ degrees of latitude, and both bolometer and spectrometer were taken simultaneously. Accurate profiles from the TES spectrometer are available. In addition, The Thermal Emission Imaging System (THEMIS) (Christensen et al., 2004) onboard Mars Odyssey, which has been operational since 2001, provides retrieved column-integrated optical depth and atmospheric temperature (Smith, 2009) as validation during the bolometer-only observations.

Summary: Atmospheric aerosol and thermal properties can be retrieved from the extended bolometer-only dataset. These properties include aerosol optical depth and atmospheric temperature from limb-viewing geometry as well as surface temperature and albedo from nadir-viewing geometry. We intend to present retrievals during times when the spectrometer is operational to validate the results. This work will be extended to the TES bolometer-only observations to derive a systematic view of aerosol and thermal properties across Mars.

Bibliography:

Christensen, P.R., et al., 1992. Thermal Emission Spectrometer Experiment: Mars Observer Mission, *J. Geophys. Res.,* 97, 7719-7734.

Christensen, P.R., et al., 2001. Mars Global Surveyor Thermal Emission Spectrometer experiment: Investigation description and surface science results, *J. Geophys. Res.*, 106, 23823- 23876.

Christensen, P.R., et al., 2004. The Thermal Emission Imaging System (THEMIS) for the Mars 2001 Odyssey Mission, *Space Sci. Rev*., 110, 85-130.

Clancy, R.T., M.J. Wolff, P.R. Christensen, 2003. Mars aerosol studies with the MGS TES emission phase function observations: Optical depths, particle sizes, and ice cloud types versus latitude and solar longitude, *J. Geophys. Res.*, 106, doi:10.1029/2003JE002058.

Clancy, R.T., M.J. Wolff, B.A. Whitney, B.A. Can-

tor, M.D. Smith, T.H. McConnochie, 2010. Extension of atmospheric dust loading to high altitudes during the 2001 Mars dust storm: MGS TES limb observations, *Icarus*, 207, 98-109.

Gordon, I.E., and 54 co-authors, 2017. The HITRAN2016 molecular spectroscopic database. *J. Quant. Spectrosc. Rad. Transf.*, 203, 3–69, doi:10.1016/j.jqsrt.2017.06.038.

Kutepov, A.A., A.G. Feofilov, L. Rezac, M.D. Smith, 2008. Temperatures of Martian atmosphere in the altitude region 60-100 km retrieved from the MGS/TES bolometer infrared limb radiances, Third International Workshop on the Mars Atmosphere: Modeling and Observations, Williamsburg, Virginia.

Lacis, A.A., and V. Oinas, 1991. A description of the correlated-k distribution method for modeling nongray gaseous absorption, thermal emission, and multiple scattering in vertically inhomogeneous atmospheres. *J. Geophys. Res.*, 96, 9027–9063. Martin, T.Z., and H.H. Kieffer, 1979. Thermal infrared properties of the Martian atmosphere, *J. Geophys. Res.*, 84, 2843-2852.

McConnochie, T.M., and M.D. Smith, 2008. Vertically resolved aerosol climatology from Mars Global Surveyor Thermal Emission Spectrometer (MGS-TES) limb sounding. Third International Workshop on the Mars Atmosphere: Modeling and Observations, Williamsburg, Virginia.

Smith, M.D., 2009. THEMIS observations of Mars aerosol optical depth from 2002–2008, *Icarus, 202*, 444–452.

Smith, M.D., M.J. Wolff, R.T. Clancy, A. Kleinböhl, S.L. Murchie, 2013. Vertical distribution of dust and water ice aerosols from CRISM limb-geometry observations. *J. Geophys. Res.*, 118, doi:10.10002/jgre.20047.

Wolff, M.J., M.D. Smith, R.T. Clancy, R. Arvidson, M. Kahre, F. Seelos IV, S. Murchie, H. Savijärvi, 2009. Wavelength dependence of dust aerosol single scattering albedo as observed by the Compact Reconnaissance Imaging Spectrometer, *J. Geophys. Res.*, 114, doi:10.1029/2009JE003350.

Wolff, M. J. and Pankine, A., 2016. Limb Retrievals of TES solarband/IR data (and MCS solarband data)", American Geophysical Union, Fall General Assembly 2016, abstract id.P21B-2107.